J Bioenerg Biomembr (2008) 40:139–147
DOI 10.1007/s10863-008-9140-3

Structure of the voltage dependent anion channel: state of the art

Vito De Pinto · Simona Reina · Francesca Guarino · Angela Messina

Published online: 31 July 2008

Abstract The eukaryotic porin or Voltage Dependent Anion-selective Channels (VDAC) is the protein forming the aqueous pore channel in the mitochondrial outer membrane. It can modulate the energy-dependent metabolism of the cell forming a diffusion barrier to ions, adenine-nucleotides and other metabolites and it is probably involved in the regulation of apoptotic-relevant events. For these reasons, VDAC co-responsibility in unphysiological events leading to important pathologies such as onset or sustainment of cancer has been envisaged very early. The knowledge of the VDAC atomic structure is thus a relevant step in the design of modern drugs acting upon the mitochondrial function and its related apoptotic balance. This goal, despite many efforts, has not been gained until now. Several predictive or descriptive techniques have been employed to obtain models or representations of the pore-structure. The results obtained are reported in this review. The emerging picture arising from these many results is coherent and sufficiently informative. From these efforts it appears that VDAC is functionally monomeric but can cluster in tight but regular groups; it is asymmetric with larger exposed domains on the cytosolic side of the outer mitochondrial membrane; the diameter of the pore is between 2.5–3.0 nm and it is apparently free from obstructions (in the open state); the channel wall is mainly formed by typical amphipathic beta-strands; mobile components (the N-terminal ?) can have functional relevance to the pore regulation.

V. De Pinto (✉) · S. Reina · F. Guarino · A. Messina
Laboratory of Biochemistry and Molecular Biology,
Department of Chemical Sciences, University of Catania,
Viale A.Doria, 6,
95125 Catania, Italy
e-mail: vdpbiofa@mbox.unict.it

V. De Pinto · S. Reina · F. Guarino · A. Messina
Istituto Nazionale Biostrutture e Biosistemi,
Rome, Italy

Abbreviations

PS	phosphatidylserine
PC	phosphatidylcholine
PE	phsphatidylethanolammine
CL	cardiolipin
AFM	atomic force microscopy
VDAC	Voltage Dependent Anion selective Channel
NcVDAC	VDAC from Neurospora crassa
ScVDAC	VDAC from Saccharomyces cerevisiae
HVDAC	VDAC from human
OMM	outer mitochondrial membrane
HK	Hexokinase

Introduction

The mitochondrial outer membrane separates the intermembrane space from the cytosol. The whole exchange of metabolites, cations and information between mitochondria and the cell occurs through the outer membrane. VDACs, also known as mitochondrial porins, are the most abundant integral membrane proteins found in the outer membrane. They form the pores able to filter hydrophilic solutes up to a well-defined exclusion limit of about 3,000 Da (Colombini 1979; Benz 1994). During evolution VDACs developed as slightly basic proteins with Mr around 30 kDa. Gene duplication or other evolutionary events generated sets of porin genes in almost any organism studied so far (De Pinto and Messina 2004; Young et al. 2007). Despite the lack of definitive information and the substantial sequence conser-

vation, each VDAC isoform is suspected to have a distinct physiological role (Anflous and Craigen 2004).

The outer membrane creates a diffusion barrier for small molecules and since its permeability in particular to ATP may be modulated by up- and downregulation (closure/opening) of its conductance, VDAC has been considered the master regulator, or governator, of mitochondrial function (Lemasters and Holmuhamedov 2006). Due to its position in the cell, as the main interface between the mitochondrial and the cellular metabolisms, VDAC co-responsibility in unphysiological events leading to principal pathologies such as the onset or sustainment of cancer has been envisaged very early. There are at least three lines of evidence that suggest an important role of VDAC in pathology.

1) VDAC plays a pivotal role in the "Warburg effect", one of the oldest known metabolic phenotype of the cancer cells. VDAC is indeed the receptor of hexokinase. Thus, HK while preventing apoptosis by binding to VDAC (see review by Shoshan-Barmatz, this issue), also supports cancer cell growth by receiving preferred access to ATP newly synthesized. The binding between receptor and enzyme is reversible and modulates either the closure of the pore and the production of glucose-6-Pi, a decisive substrate for biosynthetic pathways of relevance for the cancer (Pedersen 2007).
2) Several models of outer membrane permeabilization during apoptosis represent VDAC as a key molecule in this process (Shoshan-Barmatz et al. 2006; Kroemer et al. 2007). Despite a recent report claiming that simultaneous knockout of the three VDAC genes in mouse cells does not provoke changes in the apoptotic balance (Baines et al. 2007), it is a general experience that alteration of the expression levels of VDAC(s) has a strong influence on the electrical potential of the mitochondrial membrane and thus on the cell fate through apoptosis-related mechanisms (Zaid et al. 2005; Abu-Hamad et al. 2006; De Pinto et al. 2007; Tajeddine et al. 2008; Yuan et al. 2008).
3) VDACs are considered a novel target for drugs. This experimental perspective has been pointed out by several lines of evidence. If VDAC(s) is(are) apoptosis effector(s), any molecule affecting VDAC(s) protein may have a potential role as a drug. Indeed, the main mechanism by which chemotherapeutic agents destroy cancer cells is the induction of apoptosis (Granville and Gottlieb 2003; Hail 2005).

Recently in their search for a mechanism to keep the potentially lethal proapoptotic BAX and BAK molecules in check, Cheng et al. (2003) discovered that BAK in the mitochondria of viable cells is present in complex with VDAC2. As a consequence, *VDAC2*-deficient embryonic stem (ES) cells are more sensitive to the pro-apoptotic drug staurosporine: this effect was reversed by re-expressing VDAC2 in *VDAC2–/–*ES cells. Finally Yagoda et al. (2007) discovered that erastin, a new anti-cancer compound, acts through mitochondrial VDAC: they demonstrated, using a radiolabelled analogue and a filter-binding assay, that erastin binds directly to VDAC2.

In addition, in the last years VDAC has been involved in many intra-cellular interactions and in different subcellular localizations. Among the most relevant, it was found to interact with cytoskeletal proteins (Linden and Karlsson 1996) and is to be considered a component of the gate for the Ca^{2+} trafficking (Rapizzi et al. 2002; see also review by Hajnoczky, this issue), not forgetting its localization in the plasma membrane (Baker et al. 2004).

From these quickly sketched notes it looks clear that the knowledge of the tertiary structure of the VDAC protein(s) would heavily improve our capacity to understand and interfere with critical cellular processes. Unfortunately the lack of a suitable crystal structure has hampered, until now, to achieve this goal. In this minireview we thus will synthesize the overall information, obtained with predictive and experimental approaches, available on the structure of VDAC.

Secondary structure and topology of VDAC

Predictions of the beta barrel topology

When the first VDAC primary sequences were reported (Mihara and Sato 1985; Kleene et al. 1987) the quest for the topology of the protein began. From the secondary strucure predictors available at that time (i.e. see.: Vogel and Jähnig 1986) and inspired by the crystal structure of bacterial porins, discovered within the same years, it was easy to detect the alternating hydrophilic/hydrophobic motif, typical of amphipathic beta strands arranged to form a transmembrane beta-barrel (Forte et al. 1987; De Pinto et al. 1991; Mannella et al. 1992; Rauch and Moran 1994). The presence, but not the number, of amphipathic beta strands was confirmed by applying more modern bioinformatic technologies. In a study with the Bayesian statistical algorithm called the Gibbs sampler it was found that exclusively VDAC and Tom40 were candidate for the short (11–13 residue) repetitive sequence pattern corresponding to beta strands in bacterial porins of known structure (Mannella et al. 1996). The structural similarity between the bacterial porins and the eukaryotic proteins of the outer mitochondrial membrane found with the Gibbs sampler was confirmed by Neural Network predictors. These machines are trained with sequences containing transmembrane beta-barrels (bacterial porins) and applied upon eukaryotic

proteins to look for the same kind of motifs (Diederichs et al. 1998). With this predictive method Bay and Court (2002) identified in NcVDAC eight cytoplasmic and seven IMS loops, generating a predicted topology of 16 beta strands.

A further application of Neural Network predictors was reported by Casadio et al. (2002). A set of three specialized Neural Network predictors, trained upon membrane beta strands, globular or membrane α-helices was employed to scan the VDAC1 sequence in different eukaryotic organisms. In particular a neural network predictor specifically suited to localise the position of β strands of outer membrane proteins was used. This predictor localised 16 β strands along the sequence. The other predictors detected only minor helical stretches and not one of them was able to cross the membrane. Modelling of VDAC was then performed aligning the prediction to the templates based on secondary structure. As a template three bacterial porins (2OMF, 1PRN and 2POR) were used, each of them sharing a 16 β transmembrane strand structure, but with very low sequence identity (below 30%). Gaps were confined to the loop regions: this was necessary since loops in the bacterial porins are longer than those in the VDACs. The best alignment was the model that had the best PROCHECK (Laskowski et al. 1993) score (minimum percentage of residues in disallowed conformation). The overall result was the first 3D prediction of a eukaryotic porin or VDAC. The evaluation results indicated that the models were characterised by a percentage of residues in allowed regions comparable with that of a crystal with a resolution <0.2 nm (Casadio et al. 2002) (Fig. 1).

Secondary structure predictions on a multi-alignment of 244 VDAC proteins were recently performed with SSPRO v.2 (Poliastri et al. 2002), another neural network software. It was able to localize a general pattern with 19 regions showing strand propensity (Young et al. 2007). Some of them were ambiguous, like the β strands 8/9, or predicted only in plant or fungi or too short to cross the membrane (for a complete discussion see Young et al. 2007). As a result, their most probable model would include 16 β strands.

Various experimental strategies were used to validate theoretical predictions of the transmembrane topology of VDAC, or even to guide the construction of VDAC models. Proteases and peptide-specific antibodies contributed to define the topology of VDAC (De Pinto et al. 1991; Stanley et al. 1995). These large molecules could identify exposed domains of the pore, instead of the channel-forming structure. A specific monoclonal antibody confirmed the presence of the N-terminal end outside the membrane, since it was labelled strongly in mitochondria (see below). Other antibodies identified beta strand-connecting loops (Stanley et al. 1995). The proteolytic strategy was also applied to intact mitochondria and the resulting peptides were detected with antibodies: in this way some

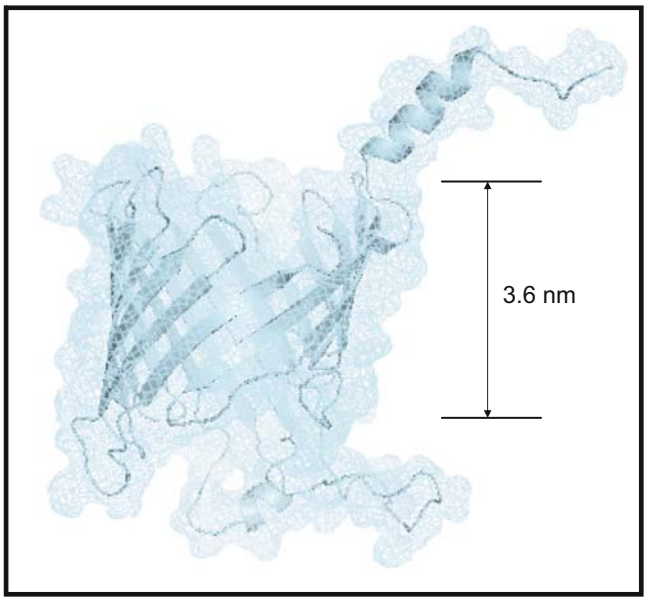

Fig. 1 Three-dimensional hypothetical model of HVDAC1. The model consists of a β barrel containing 16 β strands and a α helix sketched using PyMOL v1.0. The conformation of the amino acids at the N-terminal region of the protein was predicted by SSP4 fold recognition server. The *arrow* indicates a distance of about 3.6 nm. Courtesy of Andrea Guarnera (Catania, Italy)

putative cleavage sites were assigned on the basis of the peptide masses estimated by electrophoresis (De Pinto et al. 1991). Recently Engelhardt et al. (2007) updated this approach using recombinant, refolded HVDAC1 in detergent micelles. They were able to detect several proteolytic sites by applying more modern techniques like MALDI-MS analysis of peptides. Together with a bioinformatic secondary structure prediction, these results produced a new topology diagram with 16 β strands (Engelhardt et al. 2007).

Another line of experiments used site-directed mutagenesis, expression of the mutants and functional characterization to assess the role of selected amino acids in the sequence. The rationale of this strategy resides in the idea that replacement of hydrophilic amino acid residues is important when it affects electro-physiological features of the reconstituted channel. The portions of the protein that face the ion stream, i.e. the wall of the pore, could thus be predicted with site-directed mutagenesis. When a charge change at one site altered the selectivity of the channel in the correct direction then that site was assigned to be part of the wall of the channel (Blachly-Dyson et al. 1990; Thomas et al. 1993; Song et al. 1998a). No change in selectivity following site-directed mutagenesis was interpreted to indicate that the site of mutation did not form part of the wall. According to these experiments, topological models of VDAC were proposed. They all consider that the single, N-terminal amphipathic α-helix and 12 (Blachly-Dyson et al. 1990) or 13 β strands (Song et al. 1998a) cross the

membrane forming a barrel-like water-filled channel in the open state of the pore (Fig. 2).

The results obtained with this laborious strategy, however, contributed just another model prediction. Interestingly a critical evaluation of the mutated residues showed that the deduced localization of most of them was consistent with alternative models (Casadio et al. (2002) and Bay and Court (2002)).

The 13 β strand model, in addition to be "aesthetically unappealing" (Rostovtseva et al. 2005) is somehow unrealistic in comparison with the evolution of the transmembrane β barrel proteins known to date. The β barrel organization, at least in bacterial porins, follows few, generally, well identified rules. The relevant points are the tilting angle of the strands, the shear number, the number of strands, and the barrel radius: they are connected by simple mathematic relations (Schulz 2004). Every β barrel known has an even number of antiparallel beta strands: this is necessary to satisfy hydrogen bonding requirements and twisting stresses (Koebnik et al. 2000). Despite the fact that no evolutionary correlation can be extended from prokaryotic to eukaryotic pore-forming proteins it is likely that the similar problem of approaching, folding and span the outer membrane in a organelle or organism surrounded by a double membrane was solved by evolution with a similar tool: this gives a conceptual appeal to the 16-beta strand models until the structure of these pores will be solved.

Importance of the N-terminal region of VDAC

Since its primary sequence was determined, the N-terminal end of VDAC was predicted to contain an amphipatic α-helix (Kleene et al. 1987). This structure represents an addition to the bacterial general porins which inspired most of the VDAC models. It is one of the most conserved sequence in VDAC (76 upon 80 animal VDAC show the same motif, Young et al. 2007). Since it is unique in the realm of transmembrane outer membrane proteins, it was the object of considerable interest and it was proposed to have functionally relevant properties (Colombini et al. 1987; Peng et al. 1992a, b; Stanley et al. 1995; De Pinto et al. 2007; Yehezkel et al. 2007). The basic questions about the VDAC1 N-terminal are: is this short sequence an α-helix and is it part of the channel wall or is it outside the membrane?

Site-directed mutagenesis showed that changes in the charge of this sequence influenced the selectivity of the channel (Blachly-Dyson et al. 1990). Furthermore it has been proposed that the N-terminus may be part of the mobile voltage sensor, the structure responsible for sensing the voltage potential across the membrane where the pore is inserted, causing its partial closure (Song et al. 1998b).

Monoclonal antibodies were prepared against the synthetic VDAC1 N-terminal sequence (Babel et al. 1991). These antibodies invariably detected this moiety outside the membrane (De Pinto et al. 1991; Stanley et al. 1995), demonstrating convincingly that in situ it is an extramembranous, exposed domain. Comparison of intact mitochondria with mitochondria carrying a damaged outer membrane, showed that only in the former situation is there an access to the epitope, proving its inter membranous localization (Konstantinova et al. 1995; Stanley et al. 1995).

The structure of the N-terminus has been recently determined by NMR (De Pinto et al. 2007). The 19-mer

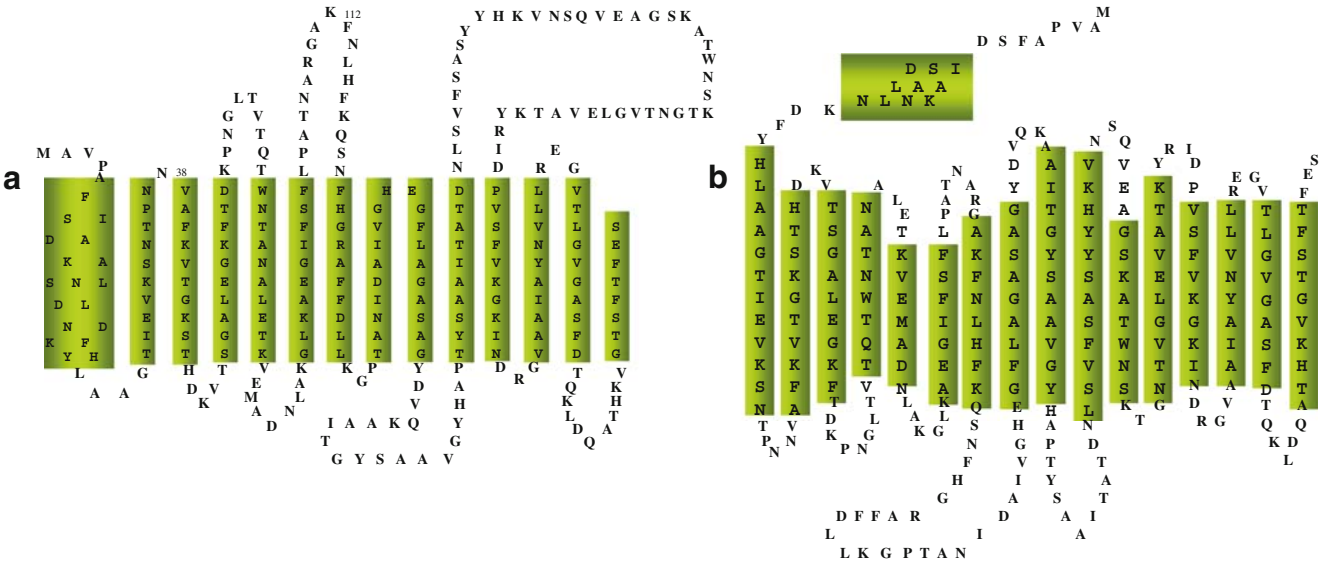

Fig. 2 Current topological models of *N. crassa* VDAC. Ribbons indicate β strands and a cylinder indicates the N-terminal α helix. **a** The 13 β strands/one α helix barrel-forming model designed in Song et al. (1998a). **b** The 16 β strands barrel-forming model in the topology reported by Casadio et al. (2002)

HVDAC1 N-terminal acetylated peptide encompassing the 2–20 amino acids sequence predicted to constitute the N-terminal α-helix of the VDAC protein was synthesized. The peptide's secondary structure was determined with CD and NMR spectroscopy, under different experimental conditions. Chemical shift values and the NOE connectivities obtained in the membrane-mimicking environment generated by SDS micelles, support the presence of a helical segment spanning residues T5-V16. The presence of two proline residues hampers the very N-terminus to be involved in the helical structure. Interestingly the helical region does not span the whole peptide sequence but only part of it, in good agreement with predictions (Casadio et al. 2002; Young et al. 2007). Thus a α-helix formed by 11 residues is too short to cross a whole membrane, as required by some models (Rostovtseva et al. 2005).

An extensive circular dichroism spectropolarimetric analysis of the peptide revealed interesting features: this amino acid stretch forms a secondary structure only in a specific environment. As preliminarly shown by Guo et al. (1995) the highest alpha-helical content is obtained in SDS, while in water the peptide is random coil (De Pinto et al. 2007). A further insight came from CD spectra in the presence of the non-ionic detergent dodecil-β-maltoside: in this context the peptide was again unstructured, clearly showing that the micellar environment is not sufficient to force the peptide into the helical conformation. This observation has been deepened by differential scanning calorimetric experiments aiming at define the interaction of the peptide with the membrane. The interaction of the VDAC1 N-terminus peptide with a membrane formed by a zwitterionic phosholipid (PC) was negligible; on the other hand, when a negatively charged phospholipid (PS) was used in the host membrane, the thermally-induced transition of the lipid bilayer was affected by the presence of the peptide. The quality of the interaction indicates that the peptide did not insert deep into the membrane but, instead, interacted with its surface. Most important, CD spectra recorded in the presence of PC revealed that it had a random coil structure while with PS the typical alpha-helical content was observed (De Pinto et al. 2007). The conclusion is that the N-terminus end of VDAC needs a hydrophobic and negatively charged environment to gain its α-helical structure.

Rostovtseva et al. (2006) studied the influence of the lipid membrane composition upon the asymmetry of the VDAC gating. They found that VDAC gating is symmetrical in membranes made of PC or PC:PE (1:1) but becomes asymmetrical in membranes containing only PE or cardiolipin in PC (CL:PC=4%). PC has a small negative spontaneous curvature, while PE and CL have a high negative spontaneous curvature. This means that the lipid composition of the membrane has an effect on the VDAC state and that such an effect is related to the elastic stress of lipid packing (Rostovtseva et al. 2006). The VDAC-gating is a transition between the open and closed state of the pore: this transition should cause conformational rearrangements of the protein (Peng et al. 1992a). The surprising finding was that 4% CL in PC membranes caused a strong asymmetry in VDAC-gating and that this effect is specific for VDAC since gramicidin channels were affected only slightly by CL. The authors hypothesize that this effect can be accounted for by a predominant VDAC insertion in CL-rich membrane domains or by a non-specified influence on VDAC channel gating. At this point it is worthwhile to remember that CL carries negative charges and that the N-terminus end of VDAC needs the presence of a negatively charged hydrophobic milieu to form an α-helix. Thus can CL provide the right environment for the interaction of the N-terminus (or the voltage sensor) with the membrane?

The lipid composition of the mitochondrial membranes has been investigated in details in past years. De Kroon et al. (1997) for example, found by chromatographic methods that the outer mitochondrial membrane contains as little (<0.1%) PS as any other membrane. This phospholipid has been used in the DSC experiments to mimic the presence of negative charges in the hydrophobic milieu where the peptide was inserted (De Pinto et al. 2007). Cardiolipin is rather scarce in the lipid composition of the mitochondrial outer membrane (3–4% of lipid weight, Ardail et al. 1990; De Kroon et al. 1997). Nevertheless its rise to 20% of the total lipids in contact sites, points of close proximity between the inner and the outer membrane (Ardail et al. 1990). Contact sites are enriched in VDAC (Crompton 1999) and are candidate sites for the presence of the Transition Pore, that could contain VDAC as the outer membrane component (Kroemer et al. 2007).

The functional importance of the N-terminal region of VDAC1 has been demonstrated. Partial or complete deletion of this sequence causes modification in the electrophysiological activity of the porin (Popp et al. 1996; Koppel et al. 1998) (Fig. 3). In cells overexpressing N-terminally-truncated VDAC1, a decrease in the membrane depolarization (De Pinto et al. 2007) was observed upon induction of apoptosis by various stimuli. On the other hand its deletion appears to be ininfluent upon the mitochondrial targeting of the protein (De Pinto et al. 2007).

The structure of VDAC in the membrane

Shape of the mitochondrial outer membrane VDAC channel

In *Neurospora crassa* the abundance of VDAC allows the formation of two-dimensional crystals of the protein upon

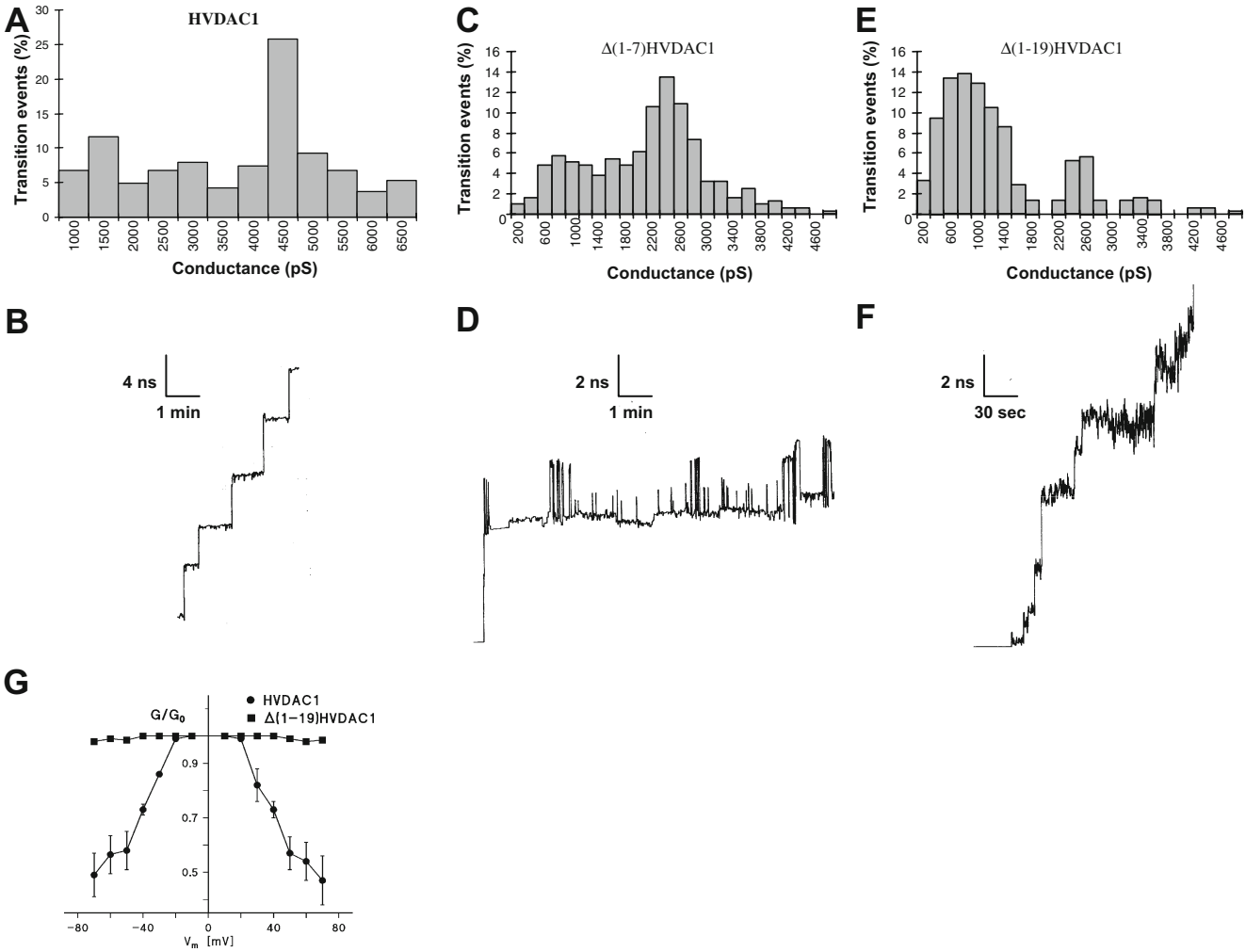

Fig. 3 Electrophysiological features of HVDAC1 and its N-terminal deleted mutants. Recombinant HVDAC1 and its mutants Δ(1–7) HVDAC1 and Δ(1–19)HVDAC1 were refolded and studied in black lipid bilayer membranes. The deletion of the amino acids 1–19, i.e. the whole sequence forming the N-terminal region (De Pinto et al. 2007), resulted in a protein whose pore-forming activity was heavily affected (**e**–**g**). **a** Histograms from single channel recordings of recombinant HVDAC1 carrying a 6×His tag. Data were obtained in 1.0 mol dm^{-3} KCl and at 20°C. At least 200 events were recorded for each protein. **b** Single channel recording of recombinant HVDAC1 in 1 mol dm^{-3} KCl at 20°C. **c** Histograms from single channel recordings of recombinant Δ(1–7)HVDAC1. Conditions as in **a**. **d** Single channel recording of recombinant Δ(1–7)HVDAC1. Conditions as in **b**. **e** Histograms from single channel recordings of recombinant Δ(1–19)HVDAC1. Conditions as in **a**. **f** Single channel recording of recombinant Δ(1–19)HVDAC1. Conditions as in **b**. **g** Voltage dependence G/G_0 of recombinant HVDAC1 and Δ(1–19)HVDAC1. Each point is the ratio between the membrane conductance (G) at the indicated voltage and the initial value of the conductance (G_0, which was a linear function of the voltage) obtained immediately after the onset of the voltage. *Open triangles* represent HVDAC1, *solid squares* Δ(1–19)HVDAC1. Points were mean±SE. (with permission from De Pinto FEBS Letter, vol 520 p. 1, 2002.)

treatment of mitochondrial outer membranes with phospholipase A^2 (Mannella 1984). This phenomenon was exploited by the group of Mannella. They reported various studies on *N. crassa* porin channel and produced the only images available, until recently, of the pore in vivo. Projection images of VDAC arrays have been obtained by electron microscopy (EM) and correlation averaging. Averaging independent channels at a considerably high resolution (2 nm) allowed the reconstruction of a single-pore 3-D image (Guo et al. 1995). From EM of 2-D fungal VDAC crystals a projected density map of the lumen of NcVDAC and a 3-D shape of the inner wall of the pore was obtained (Mannella 1998). The number and tilt of β strands was unpredictable from the EM images. Guo et al. (1995) noticed that sectors of the lumen wall are shorter than the width of a phospholipid bilayer: this justifies the observation that beta strands may have different lengths (Casadio et al. 2002).

The interaction of Fab fragments derived from antibodies specific for residues 1–20 of NcVDAC with 2D crystals of the channel was studied further. The immunochemical binding was visualized at a corner of the unit cell,

extending laterally out from the lumen. The authors suggested that the results obtained are consistent with the α-helical structure projecting laterally away from the pore. The "flap" was depicted in a three-dimensional reconstruction of the pore as a result of gold–glucose embedding (Guo et al. 1995). In the same reconstruction this "flap-like region" occurs close to an area of absence of mass (groove) suggesting that the N-terminal region might be a mobile component of the pore, involved in the process of gating. According to this work, the N-terminal may either move to the surface of the lumen or move inside the lumen. It is unlikely that it could extend vertically into the aqueous medium as a helix, since it is uncoiled in water (De Pinto et al. 2007). The same authors compared their 3-D reconstruction with the atomic-resolved structure of bacterial porin. Mannella (1997) superimposed the C-alpha backbone of *Rhodobacter capsulatus* porin on an outline of the VDAC lumen as derived from image-reconstruction of *Neurospora* crystals. The fit between the *Rhodobacter* porin backbone and the VDAC outline was surprisingly good (Mannella 1997).

In the absence of suitable 3-D crystals, atomic force microscopy was recently applied to preparations of the outer membrane (Gonçalves et al. 2007; Hoogenboom et al. 2007). The topographs of yeast mitochondrial outer membrane in physiological buffer, under conditions close to native, showed a surprisingly beautiful view of a pierced surface crowded with holes at least 2 nm deep, the maximum depth that the AFM tip could enter in (Gonçalves et al. 2007). Hollow cylinders were visualized with variants of the same technique onto outer membrane preparations from potato mitochondria (Hoogenboom et al. 2007). AFM analysis confirmed the earlier observation of Mannella et al. (1992) that VDAC was inserted into the membrane asymmetrically. A protrusion of about 1 nm above the plane of the membrane was observed on the cytosolic side, while the intermembrane side was just flat showing the holes in it (Hoogenboom et al. 2007). This finding fits very well with topologies where long loops alternate with short turns on the opposite sides of the protein (i.e.: Casadio et al. 2002; Bay and Court 2002; Engelhardt et al. 2007). By comparison, the surface of the bacterial general porin OmpF is highly corrugated and the pore-mouth not visible, since it is hidden by the large loops (Muller and Engel 1999).

Project density maps of frozen-hydrated VDAC arrays obtained with low-dose electron microscopy yielded an approximately right-circular cylinder with a mean diameter of VDAC's pore at the C-alpha backbone of about 3.0 nm (Guo et al. 1995). The channel reconstruction did not form an ideal annular cylinder (Mannella 1998) but the lumen was observed to be more round than in the highly elliptical bacterial pores. The shape of the pore predicted in the 3-D reconstruction produced by Casadio et al. (2002) varied slightly along the sequences: it was found to be circular for *Neurospora* and mouse and slightly oval for yeast. Average values of 3 and 2.5 nm were found for the external and internal diameters of the channel, respectively (Casadio et al. 2002). AFM topographs gave a round shape and an inner diameter of 2.7 (+/−0.4) nm (Hoogenboom et al. 2007). Thus a general agreement concerning the shape and the size of the pore has been found with the techniques presently available. The estimated diameter of the pore is readily comparable to the permeability characteristics of the pore (Benz 1994, Rostovtseva et al. 2005). This diameter corresponds to those found at the C-alpha backbone of bacterial general porins (Schulz 2004). In this latter case, however, a restriction due to the folding of loop 3 inside the channel reduces the space available for the ion flow. Bacterial porins are in general about one third longer than VDACs: the additional amino acids form long loops outside the barrel. The screening properties and the structural robustness found in bacterial porins are not essential for the mitochondrial protein. Eukaryotic VDACs form pores adapted to a less selective traffic across an intracellular membrane. In the eukaryotic VDAC shorter sequences can form barrels with the same diameter, but accessible to larger molecules, than in gram negative bacteria.

Oligomeric state of VDAC

Since the earliest observations of the 2-D crystalized outer membrane it was noticed that VDAC pores organize in ordered arrays each holding six channels (Mannella 1984). A fine description of the packing of the six pores, obtained by comparison of the frozen-hydrated crystals and auro-thioglucose embedded images with low dose EM, was reported in Guo et al. (1995). From these images it was noticed that the density of the pore wall is not constant but shows four sites of below-average density in the wall, possibly due to the topology of the protein. The packing geometry of the six channels in the unit cell was also described. Interchannel contacts, i.e. places in the outer face of the channel that are the preferential sites for a contact between channels were evidenced (Guo et al. 1995). In the same work the N-terminal lateral projection was observed (see above). It is interesting to notice that the N-terminal structure always protrudes towards the outside of the packed units.

The aggregation state of VDAC was studied with biochemical cross-linking strategies resulting in various multimeric forms (Zalk et al. 2005; Malia and Wagner 2007). A tetrameric aggregate was proposed to form in vivo in pro-apoptics events (Zalk et al. 2005). An early proposal of a dimeric organization of the functional unit, deduced by

the hydrodynamic properties of the detergent-solubilized protein (Linden and Gellerfors 1983) was later corrected and the functional unit of the VDAC channel is generally considered to be a monomer (Peng et al. 1992b; Rostovtseva et al. 2000). The supra-molecular assembly of VDAC was recently studied in the OMM, using high-resolution AFM (Gonçalves et al. 2007; Hoogenboom et al. 2007). AFM topographs showed VDAC in the yeast OMM to be packed either at a high density (<80% of the surface), and at a low density (Gonçalves et al. 2007). In these topographs the pores appeared as a single molecule to groups comprising up to 20 VDAC molecules (Gonçalves et al. 2007). In isolated OMM from potato, pores were revealed as monomers or grouped in tetramers, hexamers and higher oligomers (Hoogenboom et al. 2007). The spatial arrangement of VDAC detected by AFM reminds one of the ordered packed arrays first detected by Mannella (1984) in *N. crassa* OMM. The reason of these supra-molecular organizations is as yet unknown. It may be just the result of a spontaneous aggregation of the channels due to specifically sticky sides (see the packing description in Guo et al. 1995). On the other side it could have a functional meaning: it could be important for intermembrane communication, as shown for mitochondria and ER membranes (Rapizzi et al. 2002). Furthermore it was suggested to form a grid pattern where hexokinase or other proteins could find a docking site (Hoogenboom et al. 2007).

Conclusions

In this paper we have reviewed the information available up to date about the structure of the eukaryotic porin or VDAC. All available techniques were applied to describe this structure, which proves the importance of this molecule.

There seems to be a general consensus about some features of the pore structure: it is a functional monomer that can cluster in tight but regular groups; it is asymmetric with larger exposed domains on the cytosolic side of the outer mitochondrial membrane; the diameter of the pore is between 2.5–3.0 nm and it is apparently free from obstructions (in the open state); the channel wall is mainly formed by typical amphipathic beta-strands; mobile components (the N-terminal ?) can have functional relevance on the pore.

The solution of the VDAC structure at an atomic level, which is of high urgency, still awaits suitable crystals. There are now available several procedures leading to large amounts of recombinant VDAC claimed to have the same properties as the native protein (Malia and Wagner 2007; Engelhardt et al. 2007; Bay et al. 2008): these preparations could well be the basis for new crystallization efforts. One should remember the specificity of VDAC in comparison with bacterial porins that proved to be reasonably easy to crystallize. The reason of the well-known difficulty in getting ordered crystals of VDACs could be due to an excess of mobility in some part of the molecule. The N-terminal sequence of VDAC is a likely candidate as a mobile component of the structure due to its ability to switch between alternative secondary structures (De Pinto et al. 2007). Crystallization experiments should well take this point into account.

Fifteen years ago a review published in this same journal was entitled “toward the molecular structure of the mitochondrial channel, VDAC” (Mannella et al. 1992): today we can only repeat that the full knowledge of the structure of this crucial protein is still on the way.

Acknowledgments The authors acknowledge the financial support of FIRB RBNE03PX83 and University of Catania. F.G. is a recipient of a fellowship by Istituto Nazionale Biostrutture e Biosistemi.

VDP thanks Dr. Benz (Wuerzburg, Germany) for the electrophysiological measures.

References

Abu-Hamad S, Sivan S, Shoshan-Barmatz V (2006) Proc Natl Acad Sci U S A 103:5787–5792

Anflous K, Craigen WJ (2004) In: Benz R (ed) Bacterial and eukaryotic porins. Wiley, Weinheim, pp 285–307

Ardail D, Privat JP, Egret-Charlier M, Levrat C, Lerme F, Louisot P (1990) J Biol Chem 265:18797–18802

Babel D, Walter G, Götz H, Thinnes FP, Jürgens L, König U, Hilschmann N (1991) Biol Chem Hoppe-Seyler 372:1027–1034

Baines CP, Kaiser RA, Sheiko T, Craigen WJ, Molkentin JD (2007) Nat Cell Biol 5:550–555

Baker MA, Lane DJ, Ly JD, De Pinto V, Lawen A (2004) J Biol Chem 279:4811–4819

Bay DC, Court DA (2002) Biochem Cell Biol 80:551–562

Bay DC, O'Neil JD, Court DA (2008) Biophys J 94:457–468

Benz R (1994) Biochim Biophys Acta 1197:167–196

Blachly-Dyson E, Peng SZ, Colombini M, Forte M (1990) Science 247:1233–1236

Casadio R, Jacoboni I, Messina A, De Pinto V (2002) Febs Lett 520:1–7

Cheng EH, Sheiko TV, Fisher JK, Craigen WJ, Korsmeyer SJ (2003) Science 301:513–517

Colombini M (1979) Nature 279:643–645

Colombini M, Yeung CL, Tung J, König T (1987) Biochim Biophys Acta 905:297–286

Crompton M (1999) Biochem J 341:233–249

De Kroon AIPM, Dolis D, Mayer A, Lill R, de Kruijff B (1997) Biochim Biophys Acta 1325:108–116

De Pinto V, Messina A (2004) In: Benz R (ed) Bacterial and eukaryotic porins. Wiley, Weinheim, pp 309–337

De Pinto V, Prezioso G, Thinnes F, Link TA, Palmieri F (1991) Biochemistry 30:10191–10200

De Pinto V, Tomasello F, Messina A, Guarino F, Benz R, La Mendola D, Magri A, Milardi D, Pappalardo G (2007) Chembiochem 8:744–756

Diederichs K, Freigang J, Umhau S, Zeth K, Breed J (1998) Protein Sci 7:2413–2420

Engelhardt H, Meins T, Poynor M, Adams V, Nussberger S, Welte W, Zeth K (2007) J Membr Biol 216:93–105

Forte M, Guy HR, Mannella CA (1987) J Bioenerg Biomembr 19:341–350
Gonçalves RP, Buzhynskyy N, Prima V, Sturgis JN, Scheuring S (2007) J Mol Biol 369:413–418
Granville DJ, Gottlieb RA (2003) Curr Med Chem 10:1527–1533
Guo XW, Smith PR, Cognon B, D'Arcangelis D, Dolginova E, Mannella CA (1995) J Struct Biol 114:41–59
Hail N Jr (2005) Apoptosis 10:687–705
Hoogenboom BW, Suda K, Engel A, Fotiadis D (2007) J Mol Biol 370:246–255
Kleene R, Pfanner N, Pfaller R, Link T, Sebald W, Neupert W, Tropschung M (1987) EMBO J 6:2627–2633
Koebnik R, Locher KP, Van Gelder P (2000) Mol Microbiol 37:239–253
Konstantinova SA, Mannella CA, Skulachev VP, Zorov DB (1995) J Bioenerg Biomembranes 27:93–99
Koppel DA, Kinnally KW, Masters P, Forte M, Blachly-Dyson E, Mannella CA (1998) J Biol Chem 273:13794–13800
Kroemer G, Galluzzi L, Brenner C (2007) Physiol Rev 87:99–163
Laskowski RA, MacArthur MW, Moss DS, Thornton JM (1993) J Appl Crystallogr 26:283–291
Lemasters JJ, Holmuhamedov E (2006) Biochim Biophys Acta 1762:181–190
Linden M, Gellerfors P (1983) Biochim Biophys Acta 736(1):125–129 (Dec 7)
Linden M, Karlsson G (1996) Biochem Biophys Res Commun 218:833–836
Malia TJ, Wagner G (2007) Biochemistry 46:514–525
Mannella CA (1984) Science 224:165–166
Mannella CA (1997) J Bioenerg Biomembranes 29:525–531
Mannella CA (1998) J Struct Biol 121:207–221
Mannella CA, Forte M, Colombini M (1992) J Bioenerg Biomembranes 24:7–19
Mannella CA, Neuwald AF, Lawrence CE (1996) J Bioenerg Biomembranes 28:163–169
Mihara K, Sato R (1985) EMBO J 4:769–774
Muller DJ, Engel A (1999) J Mol Biol 285:1347–1351
Pedersen P (2007) J Bioenerg Biomembranes 39:211–222
Peng S, Blachly-Dyson E, Forte M, Colombini M (1992a) Biophys J 62:123–131
Peng S, Blachly-Dyson E, Colombini M, Forte M (1992b) J Bioenerg Biomembranes 24:27–31
Poliastri G, Przybylski D, Rost B, Baldi P (2002) Proteins 47:228–235
Popp B, Court DA, Benz R, Neupert W, Lill R (1996) J Biol Chem 271:13593–13599
Rapizzi E, Pinton P, Szabadkai G, Wieckowski MR, Vandecasteele G, Baird G, Tuft RA, Fogarty KE, Rizzuto R (2002) J Cell Biol 159:613–624
Rauch G, Moran O (1994) Biochem Biophys Res Comm 200:908–915
Rostovtseva TK, Liu TT, Colombini M, Parsegian VA, Bezrukov SM (2000) Proc Natl Acad Sci U S A 97:7819–7822
Rostovtseva TK, Tan W, Colombini M (2005) J Bioenerg Biomembranes 37:129–142
Rostovtseva TK, Kazemi N, Weinrich M, Bezrukov SM (2006) J Biol Chem 281:37496–37506
Schulz GE (2004) In: Benz R (ed) Bacterial and eukaryotic porins. Wiley, Weinheim, pp 25–40
Shoshan-Barmatz V, Israelson A, Brdiczka D, Sheu SS (2006) Curr Pharm Des 12:2249–2270
Song J, Midson C, Blachly-Dyson E, Forte M, Colombini M (1998a) J Biol Chem 273:24406–24413
Song J, Midson C, Blachly-Dyson E, Forte M, Colombini M (1998b) Biophys J 74:2926–2944
Stanley S, Dias JA, D'Arcangelis D, Mannella C (1995) J Biol Chem 270:16694–16700
Tajeddine N, Galluzzi L, Kepp O, Hangen E, Morselli E, Senovilla L, Araujo N, Pinna G, Larochette N, Zamzami N, Modjtahedi N, Harel-Bellan A, Kroemer G (2008) Oncogene (in press)
Thomas L, Blachly-Dyson E, Colombini M, Forte M (1993) Proc Natl Acad Sci U S A 90:5446–5449
Vogel H, Jähnig F (1986) J Mol Biol 190:191–199
Yagoda N, von Rechenberg M, Zaganjor E, Bauer AJ, Yang WS, Fridman DJ, Wolpaw AJ, Smukste I, Peltier JM, Boniface JJ, Smith R, Lessnick SL, Sahasrabudhe S, Stockwell B (2007) Nature 447:864–868
Yehezkel G, Abu-Hamad S, Shoshan-Barmatz V (2007) J Cell Physiol 212:551–561
Young MJ, Bay DC, Hausner G, Court DA (2007) BMC Evol Biol 7:31
Yuan S, Fu Y, Wang X, Shi H, Hauang Y, Song X, Li L, Song N, Luo Y (2008) FASEB J (in press)
Zaid H, Abu-Hamad S, Israelson A, Nathan I, Shoshan-Barmatz V (2005) Cell Death Differ 12:751–760
Zalk R, Israelson A, Garty ES, Azoulay-Zohar H, Shoshan-Barmatz V (2005) Biochem J 386:73–83